Anal. Bioanal. Electrochem., Vol. 15, No. 9, 2023, 726-738
https://www.doi.org/10.22034/abec.2023.708104

Analytical & Bioanalytical Electrochemistry

Full Paper

Electrochemical Measurement of B-Nicotinamide Adenine Dinucleotide by ZrO_2 Modified Carbon Paste Electrode

Mohammad Mazloum-Ardakani,* Neda Lajmorak, Zahra Alizadeh, Hamideh Mohammadian-Sarcheshmeh, Mohammad Abdollahi-Alibiek, and Bi Bi Fatemeh Mirjalili

Department of Chemistry, Faculty of Science, Yazd University, Yazd, Iran

*Corresponding Author, Tel.: +983531232222
E-Mail: mazloum@yazd.ac.ir

Received: 17 May 2023 / Received in revised form: 21 September 2023 / Accepted: 24 September 2023 / Published online: 30 September 2023

Abstract- In this research, the electrochemical performance of carbon paste electrode modified with 4-(3,5-dimethyl-1,4,7,8-tetrahydrodipyrazolo[3,4-b: 4', 3'-e] pyridin-4-yl)benzene-1, 3-diol (DBC) and zirconium dioxide nanoparticles (ZrO_2) are investigated for the electrocatalytic oxidation of β-nicotinamide adenine dinucleotide (NADH). The kinetic parameters, transfer coefficient (α), and apparent charge transfer rate constant (k_s) were obtained 0.31 and 4.83 s^{-1}, respectively by the cyclic voltammetry (CV) technique. The anodic peak potential of the DBC modifier depends on pH and has a linear range with a slope of 0.047 V/pH. Also, the performance of the modified electrode in the electrocatalytic oxidation of NADH is investigated. It was observed that in the presence of the modifier, the overvoltage related to the oxidation of NADH decreases significantly and its oxidation potential decreases by about 300 mV. Also, the diffusion coefficient (D) between the species and the electrode surface was calculated ($D=1.93\times10^{-6}$ cm^2 s^{-1}) using the chronoamperometric method. Using the differential pulse voltammetry method (DPV), the detection limit of 5.8 nM was acquired. Two linear concentration ranges of 0.01-1.0 µM and 1.0-350.0 µM for NADH were obtained. The modified electrode was used to quantitatively analyze NADH in the blood serum sample. Also, this electrode can be acceptably utilized for the simultaneous measurement of NADH and ascorbic acid species.

Keywords- Ascorbic acid; β-nicotinamide adenine dinucleotide; Carbon paste electrode; ZrO_2

1. INTRODUCTION

There are various enzymes in the human body whose activity is the responsibility of different coenzymes. One of the largest groups of redox enzymes that have been discovered so far are dehydrogenases, which require NADH coenzyme for their activity. NADH operates as a coenzyme for more than 300 dehydrogenase enzymes. As a result, its measurement as a biological species is very important. NADH with the chemical formula $C_{12}H_{28}N_7O_{14}P_2$ is a milky powder containing two nucleotides joined via their 5'-phosphate groups, with one nucleotide containing an adenine base and the other containing nicotinamide [1,2] (structure in the supplementary information Scheme 1). There are different methods to measure NADH, including fluorescence measurement, NMR spectroscopy, spectrophotometry and coulometry [3–6]. These methods have disadvantages such as being expensive and time-consuming, difficult to work with the device or method, not being accurate, lack of a wide linear concentration range, inappropriate determination due to the presence of interfering species, etc. Compared to other methods, electrochemical methods have more advantages such as more sensitivity, reproducibility, selectivity, and are more economical in terms of time and economy. However, these methods used carbon paste electrodes (CPEs), glassy carbon electrodes (GCEs), and ordinary electrodes such as Platinum, Gold, etc. that are kinetically slow and have a high overvoltage for oxidation and reduction of biological species and thus they do not have good sensitivity and selectivity. As a result, we have to modify the electrodes. The utilization of suitable organic or inorganic modifiers, as well as different kinds of nanomaterials in the construction of the sensors, can improve their performance as a result of the following effects: enhancing the electrochemical properties, including increasing the current and improving the detection limit, the effect of reducing the overvoltage by using a modifier to determine biological species, the useful operation of the modified electrode in the measuring real samples, and the possibility of identifying interfering species in measurement of biological species [7,8]. In this study, the electrochemical behavior of 4-(3,5-dimethyl-1,4,7,8-tetrahydrodipyrazolo [3,4-b: 4', 3'-e] pyridin-4-yl)benzene-1, 3-diol (DBC) modifier was examined using a CPE electrode containing zirconium dioxide nanoparticles (DBC/ZrO_2 /CPE). By examining the voltammograms of the DBC/ZrO_2 /CPE electrode at different scan rates kinetic parameters (the transfer coefficient and the apparent charge transfer rate) were estimated. Also, the electrocatalytic oxidation of NADH biological species was investigated using DBC. The chronoamperometry method was utilized to calculate the diffusion coefficient of the species on the surface of DBC/ZrO_2 /CPE electrode. Detection limit (LOD) was calculated by DPV method. This modified electrode provides the possibility of simultaneous measurement of NADH and ascorbic acid.

2. EXPERIMENTAL SECTION

2.1. Materials and apparatus

NADH was bought from Sigma Aldrich and other materials were from Merck Company. Electrochemical measurements were investigated by a potentiostat/galvanostat (SAMA 500, electro analyzer system, Iran) with a 3 electrodes system. A Metrohm 691 pH/ion meter was utilized for the pH measurements. In the purpose of material characterization, FT-IR spectra was recorded by BRUKER EQUINOX 55 single-beam spectrometer. SEM (VEGA\\TESCAN-XMU) images were recorded. XRD (X-ray diffraction) was also studied using a Philips X'Pert PRO X-ray diffraction by Cu K_{α} radiation.

2.2. Synthesis of DBC modifier

0.15 mL Hydrazine hydrate, ethyl acetoacetate (0.001 mol), 4,3-dihydroxybenzaldehyde (0.001 mol), ammonium acetate (0.004 mol), and nano-ovalbumin biocatalyst (0.05 g) were mixed and stirred at 55 °C in water (3 mL). After the completion of the reaction, the mixture was allowed to reach room temperature. Next, water (5 mL) was added. The obtained precipitations were filtered and washed first with water and acetone, respectively. To separate the catalyst, the precipitations were dissolved in N, N-dimethylformamide and filtered. By adding water to the solution under the filter with stirring, the desired product appeared as a pure precipitate [9].

2.3. Synthesis of zirconium dioxide nanoparticles

A solution of $ZrCl_4$ (1 mM, 232 mg) in distilled water (25 mL) was prepared. Then, the mixture of water and ammonia was added slowly to the solution and stirred vigorously, until the pH value became 9. To form a gel, the mixture was stirred for 24 h. The resulting gel was centrifuged and washed 5 times with 5 mL of deionized water each time and dried at 120°C for 2 h. The acquired solid was calcined for 6 h in the furnace at 350 ˚C [10,11].

2.4. Fabrication of modified electrode (DBC/ZrO_2/CPE)

DBC modifier (0.005 g) was mixed with 0.48 g of graphite powder and 0.01 g of ZrO_2 nanoparticles and mixed by grinding. Optimized amounts of DBC and ZrO_2 were obtained 1 wt% and 3 wt%, respectively (supplementary information, section 1 and 2. Figures S1-S4). Then paraffin oil was added drop by drop and mixed completely. The prepared carbon paste was inserted into a narrow glass tube with a copper wire for the electrical connection.

2.5. Characterizations

2.5.1. ZrO_2 nanoparticle characterizations

Morphology and particle size were evaluated using the scanning electron microscope (SEM) image of the ZrO_2 nanoparticles was prepared (Figure S5). This image shows spherical

nanoparticles that are attached together, and whose size is in the range of nanometers (50- 200 nm).

X-ray diffraction spectroscopy (XRD) was utilized to ensure the formation of ZrO_2 nanoparticles (Figure S6). The presence of a broad peak in the region of 24-23θ is related to amorphous zirconia. Because zirconia is calcined at 350°C and no phase change occurs at this temperature. Usually at higher temperatures (400°C), the amorphous phase turns into a mixture of tetragonal and monoclinic phases [12].

Figure S7 shows the FT-IR absorption spectrum of ZrO_2. Four peaks are observed at 480 cm^{-1}, 1370 cm^{-1}, 1455 cm^{-1}, and 1630 cm^{-1}, which are respectively attributed to Zr-O-Zr bending vibration, related to O-H-O or bond hydrogen between O-H of a Zr-OH and hydrogen of water or the O-H group of surface adsorbed water, the stretching vibration of Zr-OH and the last peaks are also related to the bending of surface adsorbed water H-O-H [13].

2.5.2. DBC modifier characterizations

The structure of DBC modifier and its characterizations, FT-IR, ^{1}HNMR, and ^{13}CNMR, were summarized in the supplementary information (section 3, Figures S8-S11).

3. RESULTS AND DISCUSSION

The DBC/ZrO_2/CPE electrochemical performance was investigated by various electrochemical techniques such as CV, DPV, and chronoamperometric in the phosphate buffer solution (0.1 M). Cyclic voltammograms by the DBC/ZrO_2/CPE electrode at various amounts of pH (3–9) at a scan rate of 100 mV s^{-1} were investigated (Figure S12). It reveals that with the increase of pH, the potential of the peaks has shifted towards more negative values. Inset (a) shows the plot of $E^{o'}$ vs. pH, which has a linear range with a slope of 46.5 mV/pH. It is almost close to the Nernst value of -59/n for a process with the same number of electrons and protons [14].

3.1. Electrochemical behavior of the modifier using DBC/ZrO_2/CPE electrode

Cyclic voltammograms of the modified electrode (CPE/DBC/ZrO_2) in the range of potential 0.0 - 0.32 V and at different scan rates (0.02-1.4 Vs^{-1}) were recorded (Figure 1). The inset (a) shows the plot of the anodic and cathodic currents versus scan rates. As can be seen, there is a linear correlation between the peak currents and the scan rates in the range of 0.02-1.4 Vs^{-1}, which reveals that the oxidation-reduction process of DBC modifier on the electrode surface is a surface-dependent process and the modifier is not under diffusion control, and the modifier is fixed on the surface of the carbon paste electrode, so the DBC modifier is connected to the electrode through surface absorption. To calculate the surface coating (Γ/mol cm^{-2}) of the electrode by DBC, the slope of the anodic and cathodic currents and the Sharpe equation (assuming the two-electron oxidation mechanism of the modifier) were applied. The amount

of Γ =5.27×10^{-8} mol cm^{-2} was obtained. In the inset (b), the potential separation of the anodic and cathodic peaks at scan rates less than 200 mV s^{-1} is insignificant, so the kinetic range of charge transfer between DBC and the electrode surface is fast. However, at scan rates higher than 200 mV s^{-1}, this separation increases, which indicates a limitation in charge transfer kinetics. At the scan rates higher than 200 mV s^{-1}, the separation of cathodic and anodic potential peak is more than 100 mV. Therefore, the necessary condition for using Laviron's theory ($\Delta E = E_{pa} - E_{pc} \geq 200/n$ mV) achieves. Using the obtained slopes from cathodic and anodic lines (in plot of potential versus log (scan rates)) and Laviron equations anodic and cathodic transfer coefficients 0.31 and 0.69, respectively were calculated. Also, apparent charge transfer rate constant (k_s=4.83 s^{-1}) was calculated [14,15].

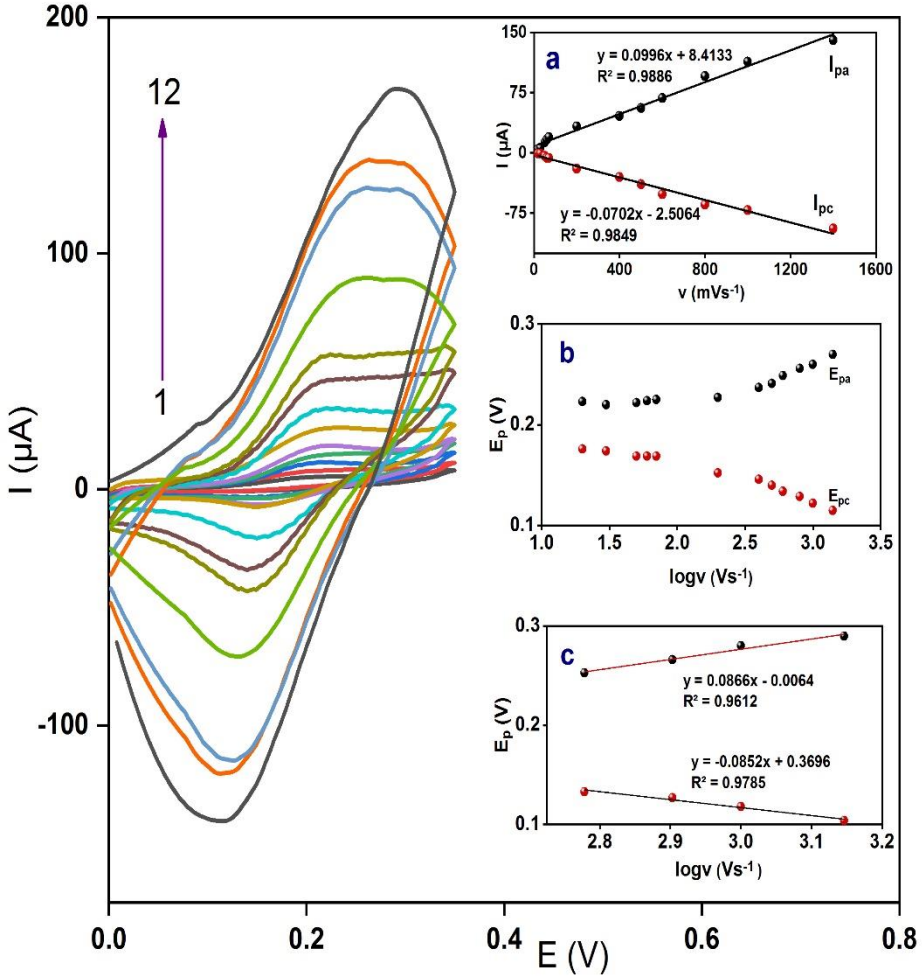

Figure 1. Cyclic voltammograms of DBC/ZrO_2/CPE electrode in 0.1M phosphate buffer solution with (pH=7.0) with different scanning rates 20, 30, 50, 60, 70, 200, 400, 500, 600, 800, 1000 and 1400 mV s^{-1}. Inset (a) changes of currents (I_p) of voltammograms against scanning rates (υ) of 20-1400 mV s^{-1}, Inset (b) plot of anodic and cathodic peak potential (E_p) against the log (υ) of 20-1400 mV s^{-1}, (c) Representing anodic and cathodic peak potential (E_p) versus the log (υ) for high scan rates (higher than 400 mV s^{-1})

3.2. Electrocatalytic oxidation of NADH on DBC/ZrO_2/CPE electrode

Cyclic voltammograms in the presence and absence of NADH species at pH=7.0 for modified and unmodified electrodes were indicated in Figure 2. Curve (a) corresponds to the unmodified CPE electrode in the buffer solution. No peak is observed in the potential range of 0.0 - 0.6 V. Curve (b) corresponds to the unmodified CPE in 0.4 mM solution of NADH. The anodic peak in the forward path is created due to the presence of NADH, but the backward peak is not observed. Curve (c) shows the carbon paste electrode modified with DBC modifier in buffer solution. The result showed that in the forward path, the anode peak is at a potential of about 0.2 V and the cathodic peak is at a potential of about 0.1 V in the backward path. Curve (d) is the modified electrode with DBC modifier and ZrO_2 nanoparticle (DBC/ZrO_2/CPE) in phosphate buffer. This curve has higher anodic and cathodic currents than voltammogram C (which only contained the DBC). Curve (e) indicates DBC /CPE electrode in 0.4 mM solution of NADH. The anodic current value in this case is higher than curve (d) (absence of NADH), and the cathodic peak is almost eliminated in the backward path. Curve (f) represents DBC/ZrO_2/CPE electrode in NADH solution. There is an anodic peak in the forward path with a higher current value compared to other curves, but the cathodic peak is almost eliminated.

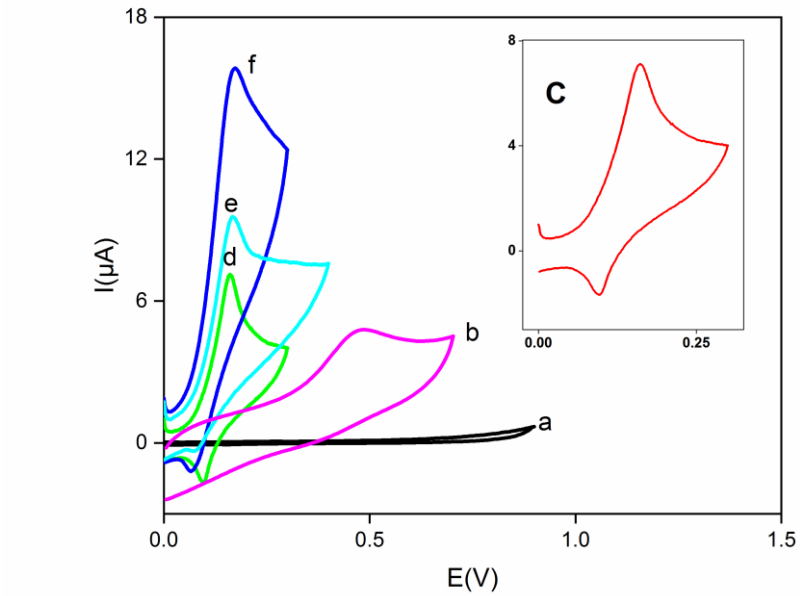

Figure 2. Cyclic voltammograms of modified and unmodified carbon paste electrodes in the presence and absence of NADH species in 0.1 M phosphate buffer solution with (pH = 7.0) at a scan rate of 20 mV s^{-1}. Inset (a) unmodified carbon paste electrode (CPE) in buffer, (b) unmodified electrode (CPE) in 0.4 mM NADH solution, (c) carbon paste electrode modified with DBC modifier (DBC/CPE) in buffer, (d) carbon paste electrode modified with DBC modifier and ZrO_2 nanoparticle (DBC/ZrO_2/CPE) in buffer, (e) DBC/CPE electrode in 0.4 mM NADH solution, (f) DBC/ZrO_2/CPE electrode in 0.4 mM NADH solution

According to the figure, it is obvious that the NADH oxidation on the surface of unmodified carbon paste electrode (b) in 0.4 mM NADH solution compared to DBC/CPE electrode (e) and DBC/ZrO_2/CPE electrode in 0.4 mM NADH solution (f) needs more overvoltage. The oxidation peak potential of NADH for unmodified electrode (b) is observed at about 490 mV, while it appears around 210 mV for modified electrodes (DBC/CPE) (e) and DBC/ZrO_2/CPE electrode (f)). It has shifted to a more negative potential approximately 280 mV. As a result, the DBC modifier has a great ability to reduce the oxidation overvoltage of NADH. By comparing of voltammogram (c) and voltammogram (e) it is observed, by adding NADH the cathodic peak current is almost eliminated and the anodic peak current is increased. This indicates a catalytic EC' mechanism. It can also be seen in the voltammogram (f) the cathodic peak current is almost eliminated and the anodic peak current increases due to the addition of NADH to the solution [7]. The presence of ZrO_2 nanoparticles improves the surface area of the electrode, thus increasing the current, measurement sensitivity and reversibility of the oxidation system and reducing the DBC modifier.

3.3. Electrochemical behavior of NADH on the surface of DBC/ZrO_2/CPE electrode

Cyclic voltammetry of DBC/ZrO_2/CPE electrode at scan rates (5.0-35 mVs^{-1}) in the presence of NADH was examined (Figure 3).

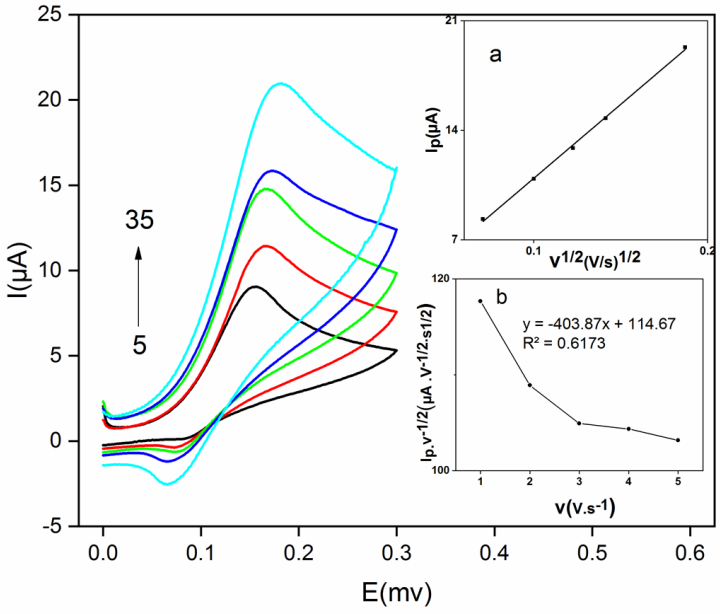

Figure 3. Voltammograms for DBC/ZrO_2/CPE electrode in phosphate buffer 0.1M with pH= 7.0 containing 0.4mM of NADH with different scan rates 5.0, 10. 0, 15.0, 20.0 and 35.0 $mV\ s^{-1}$. Inside (a) showing electrocatalytic current of NADH against the root of scanning rate ($\upsilon^{1/2}$), Inset (b) showing the normalized currents against the scan rates

Inset (a), the anodic peak current related to the oxidation of NADH species has a linear correlation with the square root of the scan rates, which reveals that the oxidation process of NADH is under diffusion control and the species reaches the electrode surface penetrates and oxidizes. Inset (b), indicates by increasing of scan rates, the value of the current function ($I_p.\upsilon^{-1/2}$) approaches a limit value. This indicates an electrochemical reaction with the EC' mechanism for oxidation of. NADH [14]. Cyclic voltammetry of the DBC/ZrO_2/CPE electrode at a scan rate of 20 mVs^{-1} using phosphate buffer solution in the presence of NADH species was studied (Figure S13). The Tafel region is highlighted in the figure. Inset (a) shows the diagram of potential versus the logarithm of the current related to the Tafel region. As can be seen, the graph is linear with a slope equal to 0.1076. Using the Tafel equation (Slope= $2.3RT/n_\alpha F$ (1-α)) and the obtained slope and considering n_α=1, the numerical value of the transfer coefficient between the DBC modifier and the NADH species was obtained (α = 0.93) [14].

3.4. Electrocatalytic oxidation of NADH by DPV method

Differential pulse voltammograms for various concentrations of 0.01-350 µM of NADH species by DBC/ZrO_2/CPE electrode were shown in Figure 4.

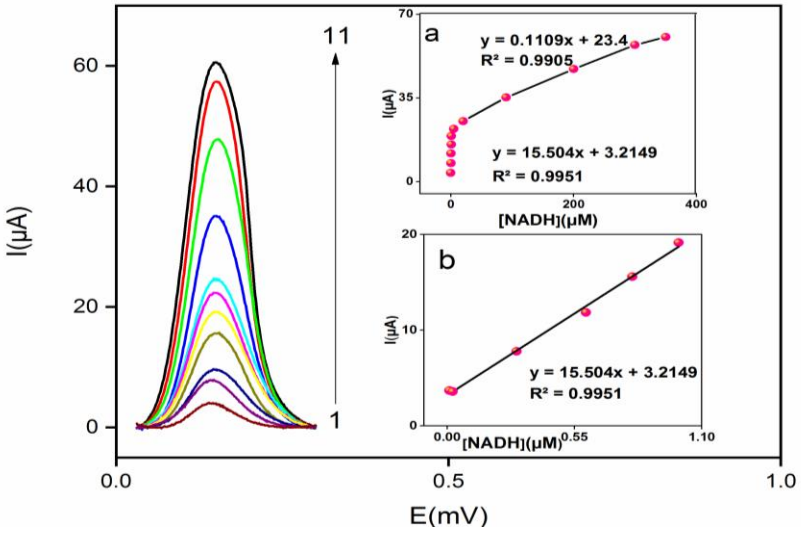

Figure 4. Differential pulse voltammograms of DBC/ZrO_2/CPE in phosphate buffer 0.1 M with pH=7.0 at a scan rate of 50 mVs^{-1} with different concentrations of NADH. The voltammograms from 1 to 11 respectively represent different concentrations of NADH: 0.01, 0.3, 0.6, 0.8, 1.0, 5.0, 20.0, 60.0, 90.0, 200.0, 300.0 and 350.0 µM NADH. Inset (a) plot of peak current versus NADH concentration in the concentration range of 0.01-350.0 µM, (b) showing the linear range corresponding to low concentrations of NADH: 0.01, 0.3, 0.6, 0.8 and 1.0 µM

The inside (a) shows the corrected current of voltammograms in the concentration range of 0.01-350 µM NADH. Inset (a) reveals two linear ranges in the calibration curve with two different slopes.

The first linear range corresponds to a concentration range of 0.01-1.0 µM with a slope of 15.504 and the second linear range corresponds to concentrations of 1.0-350 µM with a slope of 0.1109. As can be seen, the plot of current versus various concentrations of NADH species is linear which shows that the DBC/ZrO_2/CPE electrode is suitable for studying and investigating NADH in this region. To acquire the detection limit of NADH on the surface of the DBC/ZrO_2/CPE electrode, DPV were recorded in buffer solution. The standard deviation (S_b) related to the differential voltammogram currents was 0.03. Then, through the slope of the calibration curve (m) in the low concentration range and using S_b and by equation of LOD =3 S_b/m, the value of LOD was calculated as 5.8 nM.

3.5. Electrocatalytic oxidation of NADH by a chronoamperometric method

The electrocatalytic behavior of NADH was also examined using modified electrode and chronoamperometry method in a buffer solution and various concentrations of NADH (Figure S14). Inset (a) indicates the electrocatalytic current curve of NADH for DBC/ZrO_2/CPE electrode versus the inverse of the square root of time ($t^{-1/2}$) for different concentrations of NADH (0.3 mM, 0.6 mM, 0.1 mM, and 1.0 mM). A linear dependence between the electrocatalytic current and ($t^{-1/2}$) is observed, which reveals that the electrocatalytic oxidation process of NADH is under diffusion control [14]. It can also be seen that by increment of NADH concentration, the corresponding electrocatalytic current also increases. According to the mechanism of EC', by increasing the amount of NADH, more electrons participate in the reaction and increase the electrocatalytic current [16,17]. The inset (b) represents the slope of the lines obtained from (a) in different concentrations of NADH. Using these slopes and also the Cottrell equation, the value of the diffusion coefficient of NADH was obtained ($D=1.93\times10^{-6}$ cm^2 s^{-1}). Also, by the Gallus equation, the catalytic rate constant (k_h') can be calculated from the slope of lines in inset (c). It was 1.06×10^{-4} cm s^{-1} [14].

3.6. Measurement of NADH in the presence of ascorbic acid (AA)

NADH is one of the water-soluble coenzymes. The activity of more than 300 dehydrogenase enzymes depends on its presence. On the other hand, ascorbic indicates a vital role in the production of the structural proteins of the body (collagen) and its deficiency causes the weakening of the tissue structure and ascorbate disease, therefore, the measurement of this type in biological samples such as blood is so importance. In some biological samples, both of NADH and ascorbic acid are present. Because the oxidation potentials of NADH and ascorbic acid are very close to each other, it is not possible to separate these two species on the

unmodified electrode due to the overlapping of the corresponding peaks. Modified electrodes are used to solve this problem [18]. Figure S15 (supplementary information) shows the differential pulse voltammograms of DBC/ZrO_2/CPE electrode in mixtures with different concentrations of NADH and ascorbic acid. The slope of the calibration curve for NADH in the absence and presence of ascorbic acid are very close to each other (0.1149 µM and 0.1132 µM, respectively), indicating ascorbic acid has no interference in the measurement of NADH using a modified electrode (DBC/ZrO_2/CPE).

3.7. Investigating reproducibility and stability of DBC/ZrO_2/CPE electrode

In order to study the accuracy of an electrode, repeatability and reproducibility were investigated. To examine reproducibility, five DBC/ZrO_2/CPE electrodes were prepared separately and were analyzed using the DPV method in 80 µM NADH solution. A relative standard deviation percent (RSD %) of 0.8% was calculated for the response of the electrodes, which indicates the appropriate reproducibility of the DBC/ZrO_2/CPE electrode. The repeatability of DBC/ZrO_2/CPE electrode was investigated by some consecutive repeated DPV measurements in a 80 µM NADH solution. The RSD% value was 3.8%, which indicates the good repeatability of the electrode. In propose to evaluate the stability of the electrode, the differential pulse voltammogram of the electrode was compared after passing one day, three days, and one week. The RSD% values were 1.8%, 2.8%, and 3.7%, respectively, which indicates the appropriate stability of the electrode.

3.8. Interference Study

With the aim of evaluating the selectivity for the suggested method, the effect of the presence of different species on the intensity of the anodic current of NADH was examined. The range of changes was considered as the maximum concentration that causes a maximum 2% decrease or increase in the initial peak of the 80 µM solution of NADH. It was observed that if the concentration of species such as ascorbic acid, glucose, folic acid, uric acid, and tryptophan are 100 times the initial concentration of NADH, they will not have interference.

3.9. Measuring NADH in a real sample

In the aim of showing the analytical performance of the introduced sensor, measuring NADH was done in the blood serum sample. The blood serum sample was obtained from the medical diagnosis laboratory. For measuring NADH in a real sample, at first, a solution of blood serum and phosphate buffer solution with a ratio of 1:10 (1 mL of blood serum and 9 mL of 0.1 M phosphate buffer with pH = 7.0) was prepared in a volume of 10.0 mL. In the next step, different concentrations of NADH species were prepared and added to the above solution and DPVs were recorded. For each concentration of NADH, the experiment was repeated 4

times. The differential pulse voltammogram for the concentration of NADH (0.2, 0.5, and 0.9 µM) can be seen in Figure S16 (a-c). Then, by the obtained voltammogram and calibration curve equation, NADH concentrations were estimated. Also, the recovery percent related to the measurements was reported in Table 1.

Table 1. Real sample examination

Sample	Added (µM)	Obtained (µM)	RSD %	Recovery%
1	0.2	0.21	2.33	104.5
2	0.5	0.49	2.33	96.0
3	0.9	0.93	4.70	103.7
4	300.0	312.80	3.26	104.3

Table 2. Compare this work with other works

Electrode	Modifier	Analytical method	Linear range (µM)	LOD(µM)	References
GCE	rGO-AuNPs	Amp	0.05-50.0	0.0011	[19]
GCE	NiONPs	Amp	0.11-1000.0	0.1060	[23]
GCE	Gr-PQQ-CTS	Amp	0.32-220.0	0.1600	[20]
GCE	NDG	Amp	0.5-12.0	0.3700	[21]
GCE	SWCNTs(oxidized)-Polytry	Amp	0.15-83.0	0.0079	[22]
GCE	Hematoxylin	DPV	0.4-600.0	0.0800	[24]
CPE	DBC	DPV	0.01-350.0	0.0058	This work

rGO: reduced graphen oxid, **AuNPs:** gold nanoparticles, **NiONPs:** nickel oidenanoparticies, **PQQ:** Pyrroloquinolinequinone, **CTS:** chitosan. **NDG:** nitrogen doped graphene, **Polytry:**poly-tyrosine, **SWCNTs:** single walled carbon nanotubes

4. CONCLUSIONS

In this study, the electrocatalytic oxidation of NADH was evaluated by DBC/ZrO_2/CPE electrode as a modified electrode. The obtained results showed that the oxidation potential of NADH was shifted to more negative potentials around 300 mV by the modified electrode in comparison to the unmodified electrode. Some thermodynamic and kinetic parameters for NADH oxidation were calculated by electrochemical methods. Using DPV method in the concentration range of 0.01-1.0 and 1.0-350 µM, a linear correlation was observed between the intensity of the electrocatalytic current and NADH concentrations, which indicates a greater

linear range than some works [19–22] and better detection limit value in comparison to some works [20–24] according to Table 2. The modified electrode (DBC/ZrO_2/CPE) indicated the ability to separate the anodic oxidation peaks of NADH and ascorbic acid and thus simultaneous determination of two species. This electrochemical sensor could be used to measure the NADH species in real samples. This electrochemical method has major advantages in measuring NADH compared to other conventional methods such as spectroscopy and chromatography, such as the significant reduction of NADH oxidation overvoltage, good reproducibility, simple preparation of the electrode, simple and inexpensive equipment, its measurement in neutral pH (close to the pH of biological environments), a very wide concentration range for measuring NADH and no influence of interfering species in the measurement of NADH. These items highlight the application of the proposed sensor for efficient measuring of NADH.

Acknowledgments

The authors wish to thank the Yazd University Research Council for financial support of this research.

Funding

This research did not receive any specific grant from funding agencies in the public, commercial, or not-for-profit sectors.

Declarations of interest

The authors declare no conflict of interest in this reported work.

REFERENCES

[1] H.K. Chenault, and G.M. Whitesides, Appl. Biochem. Biotechnol. 14 (1987) 147.
[2] A. Bergel, J. Souppe, and M. Comtat, Anal. Biochem. 179 (1989) 382.
[3] V.P. Iordanov, G.W. Lubking, R. Ishihara, R.F. Wolffenbuttel, P.M. Sarro, and M.J. Vellekoop, Sens. Actuators A: Physical. 97 (2002) 161.
[4] M. Doverskog, U. Jacobsson, B.E. Chapman, P.W. Kuchel, and L. Häggström, J. Biotechnol. 79 (2000) 87.
[5] F. Torabi, K. Ramanathan, P.-O. Larsson, L. Gorton, K. Svanberg, Y. Okamoto, B. Danielsson, and M. Khayyami, Talanta. 50 (1999) 787.
[6] K. Umemura, and H. Kimura, Anal. Biochem. 338 (2005) 131.
[7] M. Mazloum-Ardakani, H. Mohammadian-Sarcheshmeh, A. Khoshroo, and M. Abdollahi-Alibeik, J. Anal. Sci. Technol. 8 (2017) 6.
[8] M. Mazloum-Ardakani, F. Jokar, H. Mohammadian-Sarcheshmeh, B.B.F. Mirjalili, and

S.S. Hosseinikhah, Iran. J. Anal. Chem. 8 (2021) 15.
[9] N. Salehi, and B.B.F. Mirjalili, Res. Chem. Intermed. 44 (2018) 7065.
[10] M. Mazloum-Ardakani, H. Beitollahi, M.K. Amini, F. Mirkhalaf, and M. Abdollahi-Alibeik, Anal. Methods. 3 (2011) 673.
[11] M. Mazloum-Ardakani, H. Beitollahi, M.K. Amini, F. Mirkhalaf, and M. Abdollahi-Alibeik, Sens. Actuators, B 151 (2010) 243.
[12] I.E. Sokolov, I.A. Konovalov, R.M. Zakalyukin, D. V Golubev, and A.S. Kumskov, MRS Communications 8 (2018) 59.
[13] C.O. Chikere, N.H. Faisal, P. Kong-Thoo-Lin, and C. Fernandez, Nanomaterials 10 (2020) 537.
[14] A.J. Bard, L.R. Faulkner, J. Leddy, and C.G. Zoski, Electrochemical methods: fundamentals and applications, vol 2 John Wiley & Sons, New York, NY (1980).
[15] M. Mazloum-Ardakani, A.A. Kalantari, Z. Alizadeh, H. Mohamadian-Sarcheshmeh, and H. Banitaba, Anal. Bioanal. Chem. Res. 9 (2022) 299.
[16] A.J. Bard, L.R. Faulkner, and H.S. White, Electrochemical methods: fundamentals and applications, John Wiley & Sons (2022).
[17] F. Marken, A. Neudeck, and A.M. Bond, Cyclic voltammetry, Electroanalytical Methods: Guide to Experiments and Applications (2010) 57.
[18] A. Salimi, K. Abdi, and G.R. Khayatian, Microchim. Acta 144 (2004) 161.
[19] E. Sharifi, A. Salimi, and E. Shams, Biosens. Bioelectron. 45 (2013) 260.
[20] S. Han, T. Du, H. Jiang, and X. Wang, Biosens. Bioelectron. 89 (2017) 422.
[21] S. Mutyala, and J. Mathiyarasu, J. Electroanal. Chem. 775 (2016) 329.
[22] M. Eguílaz, F. Gutierrez, J.M. González-Domínguez, M.T. Martínez, and G. Rivas, Biosens. Bioelectron. 86 (2016) 308.
[23] M. Govindhan, M. Amiri, and A. Chen, Biosens. Bioelectron. 66 (2015) 474.
[24] H.R. Zare, N. Nasirizadeh, M. Mazloum-Ardakani, and M. Namazian, Sens. Actuators B 120 (2006) 288.